

# OPTIS: a satellite-based test of special and general relativity

Claus Lämmerzahl<sup>1</sup>, Hansjörg Dittus<sup>2</sup>, Achim Peters<sup>3</sup> and Stephan Schiller<sup>1</sup>

<sup>1</sup> Institute for Experimental Physics, Heinrich-Heine-University Düsseldorf, 40225 Düsseldorf, Germany

<sup>2</sup> ZARM, University of Bremen, 28359 Bremen, Germany

<sup>3</sup> Department of Physics, University of Konstanz, 78457 Konstanz, Germany

Received 25 March 2001

## Abstract

A new satellite-based test of special and general relativity is proposed. For the Michelson–Morley test we expect an improvement of at least three orders of magnitude, and for the Kennedy–Thorndike test an improvement of more than one order of magnitude. Furthermore, an improvement by two orders of magnitude of the test of the universality of the gravitational redshift by comparison of an atomic clock with an optical clock is projected. The tests are based on ultrastable optical cavities, lasers, an atomic clock and a frequency comb generator.

PACS numbers: 0480C, 0330

(Some figures in this article are in colour only in the electronic version; see [www.iop.org](http://www.iop.org))

## 1. Introduction and motivation

Special relativity (SR) and general relativity (GR) are at the basis of our understanding of space and time and thus are fundamental for the formulation of physical theories. Without SR we cannot explain the phenomena in high-energy physics and in particle astrophysics, without GR there is no understanding of the gravitational phenomena in our solar system, of the dynamics of galaxies and of our universe, and, finally, of the physics of black holes. Both theories are linked by the fact that the validity of SR is necessary for GR.

Furthermore, new results from quantum gravity theories predict small deviations from SR and GR giving additional motivation to improve tests on SR and GR. For example, loop gravity and string theory predict modifications of the Maxwell equations [5, 6]. These modifications lead to an anisotropic speed of light and to a dispersion in vacuum, thus violating the postulates of SR. Quantum gravity also predicts, besides a violation of the weak equivalence principle [7], a violation of the universality of the gravitational redshift [8, 9]. Although the amount of SR violations predicted by quantum gravity are too small to be within the range of experimental capabilities in the near future, these predictions open up the window for violations for such

basic principles. Since we do not yet know the ‘true’ quantum gravity theory we also do not yet know the ‘true’ parameters of the theory and therefore the predicted range of violations of SR and GR is not a final prediction, but merely a hint.

Due to the overall importance of SR and GR, a persistent effort to improve the experimental tests of their foundations is mandatory. Modern tests of SR and GR using ultrastable oscillators have been performed on Earth [1–3], and an experiment is planned on the International Space Station [4].

## 2. Overview of OPTIS

By means of the proposed mission OPTIS, an improvement of three tests of SR and GR by up to three orders of magnitude is projected (see table 1).

The main features of the OPTIS mission can be seen in figure 1: a spinning drag-free

**Table 1.** Current and projected accuracies for the experiments under consideration (LPI = Local Position Invariance)

Experiment	Present accuracy	Projected accuracy
Michelson–Morley experiment (MM)	$\delta_{\theta}c/c \leq 3 \times 10^{-15}$ [1]	$\leq 3 \times 10^{-18}$
Kennedy–Thorndike experiment (KT)	$\delta_{\nu}c/c \leq 2 \times 10^{-13}$ [2]	$\leq 10^{-15}$
Universality of gravitational redshift (LPI)	$\Delta\alpha \leq 2 \times 10^{-2}$ [10]	$\leq 10^{-4}$

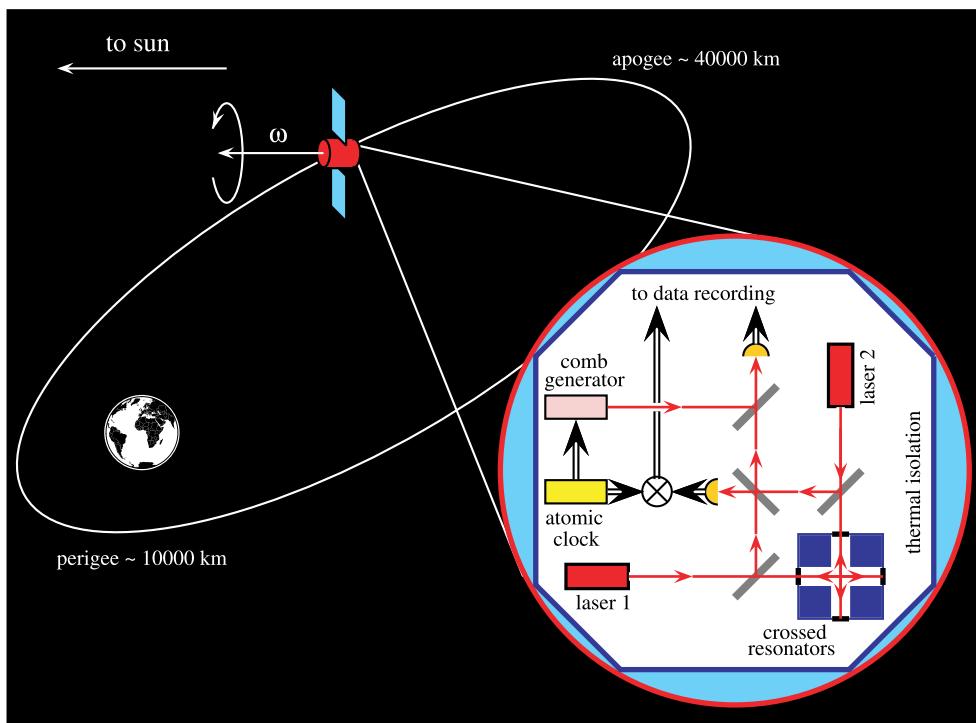


**Figure 1.** Scheme of OPTIS: the science payload of the satellite mainly consists of two crossed resonators to which two lasers are locked, an atomic clock and an optical comb generator. The orbit of the satellite is highly elliptic.

satellite orbits the Earth. The satellite payload consists of two lasers, two orthogonal optical cavities, a femtosecond laser comb generator and an atomic clock. The two cavities are used for the MM experiment which searches for differences in the velocity of light in different directions. The atomic clock represents an independent clock of different physical nature. A comparison between the atomic clock and an optical cavity can be performed by means of the comb generator. A search for a dependence of their frequency ratio with respect to a change of the velocity of the satellite or with respect to a change of the gravitational potential amounts to a KT test and to a test of the universality of the gravitational redshift, respectively.

### 3. Theoretical description and present status

The most precise experiments testing the constancy of the speed of light use cavities. The wavevector magnitude  $k$  of an electromagnetic wave in a cavity of length  $L$  is given by  $k = n\pi/L$  and the frequency  $\nu$  of an outcoupled wave by  $\nu = ck$ . If the velocity of light depends on the orientation of the cavity and on the velocity  $v$  of the laboratory,  $c = c(\vartheta, v)$ , so will the frequency  $\nu = \nu(\vartheta, v) = c(\vartheta, v)k$ . Figure 2 shows a schematic set-up for a search of an orientation and velocity dependence of the frequency. Since SR is based on an orientation- and velocity-*independent* speed of light, the search for an orientation and velocity dependence of the frequency amounts to a test of SR.

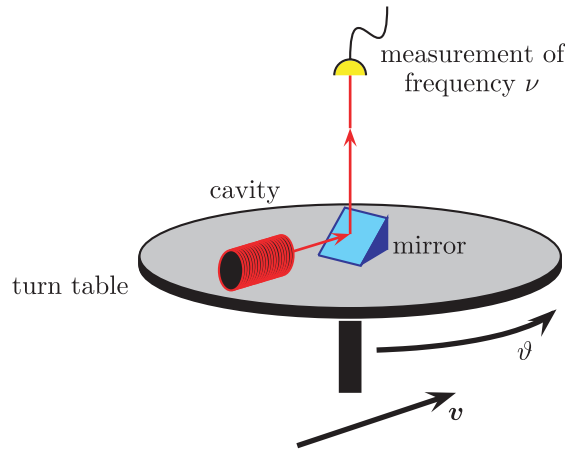


**Figure 2.** Basic set-up for a cavity experiment testing the spatial isotropy and the independence of the speed of light from the velocity  $v$  of the laboratory. If SR is valid, then the measured frequency is independent of  $\vartheta$  and  $v$ .

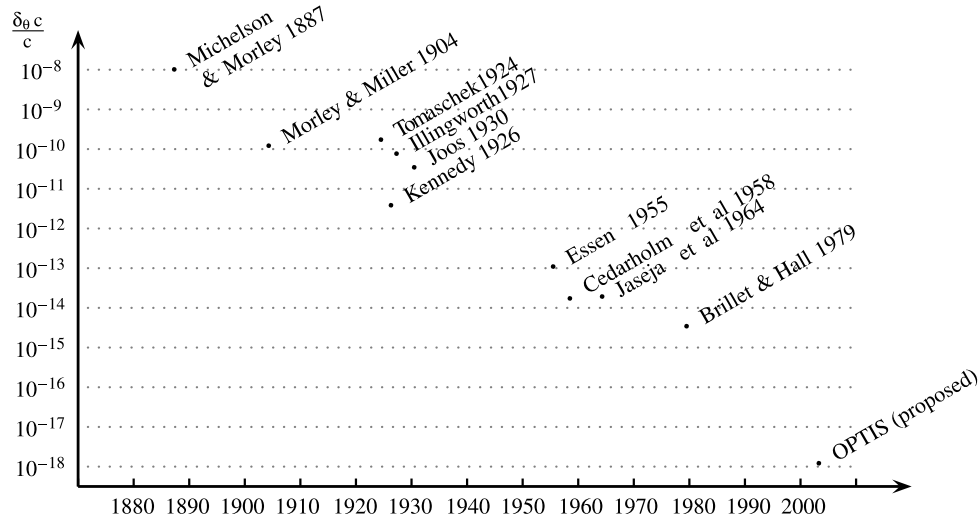
According to common test theories [11, 12], the orientation and velocity dependence of the velocity of light is parametrized according to

$$c(\vartheta, v) = c \left( 1 + A \frac{v^2}{c^2} \sin^2 \vartheta + B \frac{v^2}{c^2} + \mathcal{O}(v^4/c^4) \right). \quad (1)$$

This means that all anomalous terms vanish for vanishing velocity  $v$ . Here  $\vartheta$  is the angle between the velocity with respect to the cosmic preferred frame  $v$  and the cavity axis. In addition, an expansion with respect to  $v^2/c^2$  has been used, for simplicity. If special relativity is valid, then  $A = B = 0$ . The parameters  $A$  and  $B$  in the Mansouri–Sexl and Robertson test theories are given by table 2.

**Table 2.** Comparison of parameters in current test theories for SR.

Parameter	Robertson test theory	Mansouri–Sexl test theory
$A$	$ 1 - g_1(v)/g_2(v) $	$\beta + \delta - \frac{1}{2}$
$B$	$ 1 - g_1(v)/g_0(v) $	$\alpha - \beta + 1$

**Figure 3.** Improvements of optical tests of the isotropy of space.

### 3.1. Isotropy of space

In order to test the isotropy of space, or the isotropy of the velocity of light, one can mount the cavity on a turntable and look for a variation of the frequency as the turntable is rotated. This set-up has been used in experiments since 1955 (see figure 3). In terms of the relative variation of the velocity of light, of the Robertson parameter, and of the Mansouri–Sexl parameter, the most accurate result is [1]

$$\frac{\delta_{\vartheta} c}{c} \leq 3 \times 10^{-15}, \quad \left| 1 - \frac{g_2(v)}{g_1(v)} \right| \leq 5 \times 10^{-15}, \quad \left| \beta + \delta - \frac{1}{2} \right| \leq 3 \times 10^{-9}. \quad (2)$$

For a detailed discussion see [13].

### 3.2. Independence of the velocity of light from the velocity of the laboratory

A hypothetical dependence of the velocity of light on the velocity  $v$  of the laboratory can be tested by changing the velocity of the cavity and looking for a variation of the frequency. In Earth-based experiments, the rotation of the Earth around its axis ( $v = v_0 \pm 300 \text{ m s}^{-1}$ ) or around the Sun ( $v = v_0 \pm 30 \text{ km s}^{-1}$ ) can be used, where  $v_0 = 377 \text{ km s}^{-1}$  is the velocity with respect to the cosmic microwave background, the cosmologically preferred frame. Because of technical reasons only the rotation of the Earth around its own axis has been used so far. In terms of the same parameters as above, the most accurate result is [2]

$$\frac{\delta_v c}{c} \leq 2 \times 10^{-13}, \quad \left| 1 - \frac{g_1(v)}{g_0(v)} \right| \leq 2 \times 10^{-13}, \quad |\alpha - \beta + 1| \leq 6.6 \times 10^{-5}. \quad (3)$$

### 3.3. Gravitational redshift

Within the framework of Einstein's GR, the comparison of two identical clocks of frequency  $\nu_0$  located in different gravitational potentials  $U(x_1)$  and  $U(x_2)$  yields  $\nu(x_2) = (1 - (U(x_2) - U(x_1))/c^2) \nu(x_1)$ . The gravitational redshift does not depend on the type of clock. This is the universality of the gravitational redshift, an aspect of local position invariance.

If Einstein's theory is not correct, then the redshift may depend on the clock  $\nu(x_2) = (1 + \alpha_{\text{clock}}(U(x_2) - U(x_1))/c^2) \nu(x_1)$ , with  $\alpha_{\text{clock}} \neq 1$ . In Einstein's GR  $\alpha_{\text{clock}} = 1$ . If two different clocks are displaced together in a gravitational potential, a relative frequency shift  $\Delta\nu_{\text{clock1}}/\nu_{01} - \Delta\nu_{\text{clock2}}/\nu_{02} = (\alpha_{\text{clock1}} - \alpha_{\text{clock2}}) \Delta U/c^2$  may occur, which is proportional to the difference of the gravitational potential relative to the initial position.

For the hydrogen maser  $|\alpha_{\text{H-maser}} - 1| \leq 10^{-4}$  (GP-A experiment, [14]), verifying the gravitational redshift. For a test of the universality of the gravitational redshift by means of a comparison between a microwave cavity and an atomic caesium clock, the best result is  $|\alpha_{\text{atom}} - \alpha_{\text{cavity}}| \leq 2 \times 10^{-2}$  [3].

### 3.4. Advantages of a satellite-based test

The advantages of a satellite mission for doing experiments for testing SR and GR are the following.

- (i) The high orbital velocity (see equation (1)). For the proposed (elliptic) orbit,  $v$  varies between  $+7 \text{ km s}^{-1}$  and  $-4 \text{ km s}^{-1}$  over half the orbital period  $T_{\text{orbit}}/2 \sim 7 \text{ h}$ . This value is 20 times larger than the change of the velocity of the Earth's surface over a period of 12 h.
- (ii) The shorter period  $T_{\text{orbit}}$  of the velocity modulation as compared with 24 h on Earth. It relaxes the requirements on the optical resonators and is directly relevant for the KT and LPI tests. It is also indirectly useful for the elimination of systematic effects in the MM test.
- (iii) The difference of the gravitational potential in the highly eccentric orbit is  $\Delta U/c^2 \sim 3 \times 10^{-10}$ . This is about three orders of magnitude larger than the difference of the potential of the Sun which an Earth-bound observer experiences. This is relevant for the LPI test.
- (iv) The microgravity environment minimizes distortions of the optical resonators. This is relevant for the MM test.
- (v) A variable spin frequency of the satellite permits elimination of systematic effects.
- (vi) Long integration times (longer than 6 months).

## 4. The science payload

In this and the following section we discuss the science payload of the satellite, the relevant performance specifications and the resulting requirements for the orbit and the satellite bus structure.

In order to perform the MM test, the satellite has to spin around its axis. A typical rotation period is  $\tau_{\text{MM}} = 2\pi/\omega \sim 100\text{--}1000 \text{ s}$ . For the elimination of systematic errors, the rotation frequency  $\omega$  can be varied. For the KT test the time scale is the orbit time  $\tau_{\text{KT}} = T_{\text{orbit}} \sim 10^5 \text{ s}$ .

The main subsystems of the experimental payload are optical resonators, ultra-stable lasers, an optical frequency comb generator and an ultra-stable microwave oscillator. These components are interconnected and supplemented by the locking and stabilization electronics,

the optical bench, the drag-free control system (discussed in the next section) and an advanced thermal control system.

#### 4.1. Thermal control system

The LISA pre-phase A report [20] showed that a three-stage passive thermal isolation is sufficient to achieve a level of thermal fluctuations below  $10^{-7} \text{ K}/\sqrt{\text{Hz}}$  at  $\tau = 1000 \text{ s}$ . This performance (assuming no shadow phases) would be sufficient for the OPTIS random noise requirements. To suppress the fluctuations correlated to the rotation of the satellite, an improvement of the thermal stability by one order of magnitude would be required. This could be achieved either by an additional stage of passive isolation, or by adding active temperature stabilization.

#### 4.2. Optical resonators

The optical resonators are the central part of the experimental set-up. In the baseline configuration, two crossed standing wave resonators are implemented by optically contacting four highly reflective mirrors to a monolithic spacer block with two orthogonal holes made from a low-expansion glass ceramic (ULE, ZERODUR). With a technically feasible finesse of  $2.5 \times 10^5$  and a length of 10 cm each, these resonators should exhibit linewidths of 6 kHz.

Low-expansion glass ceramics are designed for a minimal thermal expansion coefficient ( $\lesssim 10^{-9} \text{ K}^{-1}$ ) at room temperature and can be manufactured in many different shapes and dimensions. Resonators made from these materials are well suited for laser stabilization, although ageing effects cause a continuous shrinking of the material and thereby frequency drifts of typically  $5\text{--}50 \text{ kHz day}^{-1}$ .

The monolithic construction of the resonator block serves to strongly reduce the effect of shrinking and of temperature fluctuations on the MM experiment: a high degree of common-mode rejection (two orders of magnitude) in the differential frequency measurement of the lasers locked to the resonators is expected.

For the KT and the redshift experiment, on the other hand, the ageing-related frequency drift is critical. It has to be modelled well enough to keep the unpredictable residual part below  $2 \times 10^{-13}$  (i.e. 50 Hz) over the signal half-period  $T_{\text{orbit}}/2 = 7 \text{ h}$ . This is feasible [2, 15].

For the projected measurement sensitivity the temperature stability requirements are as follows: a level  $\Delta T(\tau_{\text{MM}}) \leq 20 \mu\text{K}$  for random fluctuations over the spin period time scale and a level  $\Delta T_{\text{corr}} \leq 100 \text{ nK}$  for a temperature modulation correlated to the rotation of the satellite. For the KT as well as for the redshift experiment the requirements are  $\Delta T(\tau_{\text{KT}}) \leq 200 \mu\text{K}$  for random temperature fluctuations on a time scale of the orbit period and  $\Delta T_{\text{corr}} \leq 10 \mu\text{K}$  for temperature modulation correlated to the orbital motion.

The length of the reference resonators is affected by accelerations, with a typical sensitivity of  $1 \text{ nm g}^{-1}$  for a resonator length of 25 cm [15]. This leads to a requirement of  $6 \times 10^{-8} \text{ g}$  for random residual accelerations and  $3 \times 10^{-10} \text{ g}$  for residual accelerations correlated to the rotation of the satellite. The drag-free control system (see the next section) is designed to meet these requirements.

#### 4.3. Ultra-stable lasers

The lasers used for the OPTIS mission should have high intrinsic frequency stability, narrow linewidth and high-intensity stability. These requirements are best fulfilled by diode-pumped monolithic Nd:YAG lasers, which are also used in gravity wave detectors (GEO600, LIGO,

VIRGO, LISA) and many other high-precision experiments [16]. Such lasers are already available in space-qualified versions.

#### 4.4. Electronics for frequency and intensity stabilization

Locking the lasers to the reference resonators using the Pound–Drever–Hall frequency modulation method requires fast, low-noise photodetectors and an optimized electronic control system. The intrinsic noise of the photodetectors has to be sufficiently low to allow shot-noise limited detection. The residual amplitude fluctuations of the lasers have to be actively suppressed. To prevent thermally induced length changes of the resonators by absorbed laser radiation, the intensity of the laser beams has to be actively stabilized to a relative level of  $10^{-4}/\sqrt{\text{Hz}}$  in the frequency range 0.1 mHz to 10 Hz.

#### 4.5. Optical bench

The whole optical set-up should be stable and isolated from vibrations to prevent frequency fluctuations caused by vibration-induced Doppler shifts. Even very small displacements (less than 1  $\mu\text{m}$ ) of the laser beams relative to the reference resonators are known to cause substantial frequency shifts [17]. These requirements can be fulfilled by using a well designed monolithic optical bench on which all optical components are stably mounted as close together as possible.

#### 4.6. Atomic clock

The KT and the universality of redshift experiments require an independent frequency reference. This reference should be based on the difference of two energy levels in an atomic or molecular system. Atomic clocks based on hyperfine transitions in caesium or rubidium atoms are suited for this task. They are available in space-qualified versions with relative instabilities of better than  $1 \times 10^{-13}$  for the relevant time scale  $\tau_{\text{KT}}$  of several hours.

The atomic clock can also serve as the reference for the microwave synthesizer required to mix down the beat signal between the two stabilized lasers in the MM experiment from typically 1 GHz to a lower frequency for data acquisition and analysis. The required relative instability  $\lesssim 10^{-12}$  on the time scale  $\tau_{\text{MM}}$  of 100–1000 s is thereby satisfied.

#### 4.7. Optical comb generator

For the frequency comparison between the atomic clock and the lasers stabilized to the reference resonators it is necessary to multiply the microwave output of the atomic clock ( $\sim 10^{10}$  Hz) into the optical range ( $\sim 10^{15}$  Hz). Thanks to recent important progress in the field of frequency metrology, this can now be done reliably and simply by using femtosecond optical comb generators [18, 19]. Here the repetition rate of a mode-locked femtosecond laser of  $\sim 1$  GHz is locked to an atomic clock. Its optical spectrum (a comb of frequencies spaced at exactly the repetition rate) is broadened to more than one octave by passing the pulses through a special optical fibre. By measuring and stabilizing the beatnote between the high-frequency part of the comb and the frequency-doubled low-frequency part, it is then possible to determine the absolute frequency of each component of the comb relative to the atomic clock. In a final step the frequency of the cavity-stabilized lasers is then compared with the closest frequency component of the comb by measuring their beatnote with a fast photodetector.

Compact diode-pumped comb generators with very low power consumption, as required for space applications, are already under development.

## 5. Orbit and satellite

### 5.1. The orbit and orbit requirements

The experimental requirements define an optimum mission profile. In particular, the requirements of attitude control, maximum residual acceleration and temperature stability result in the following specifications.

- The satellite needs a drag-free attitude and orbit control system for all six degrees of freedom. Thrust control must be possible down to  $0.1 \mu\text{N}$  by means of ion thrusters (field emission electrical propulsion, FEEP).
- For drag-free control the satellite needs an appropriate reference sensor.
- FEEPs are not effective for orbit heights of less than 1000 km, because of the high gas density in lower orbits.
- To avoid charging of the capacitive reference sensor by interactions with high-energy protons, highly eccentric orbits, where the satellite passes the van Allen belt, are not appropriate.
- The KT experiment requires a low orbit, because the experimental resolution depends directly on the satellite orbit velocity.
- The precise attitude control requires a star sensor with a resolution of 10 arcsec.
- Mechanical components for attitude control (e.g. fly wheel or mechanical gyros) cannot be used, because of the sensitivity of the experiment to vibrations.
- Temperature stability requirements during integration times of more than 100 s can only be realized on orbits without any or with rare eclipse intervals.
- The thermal control of the satellite structure must achieve a stability of  $10^{-3} \text{ K}/\sqrt{\text{Hz}}$ .
- The mission time is 6 months minimum.

OPTIS is designed to be launched on a micro-satellite with limited technological performance. Considering all experimental requirements, technological feasibility, launch capability and design philosophy, the most feasible solution is to launch the satellite in a high elliptical orbit, attainable via a geo-transfer orbit (GTO) by lifting the perigee. In this scenario, the satellite is first launched as an auxiliary payload (ASAP5) by an ARIANE 5 rocket into the GTO with an apogee of 35 800 km and a perigee of only 280 km. An additional kick-motor on the satellite will lift the satellite in its final orbit with a perigee of about 10 000 km, corresponding to  $\Delta v = 0.75 \text{ km s}^{-1}$ . A minimum height of 10 000 km enables one to use ion thrusters (FEEPs) and avoids flying through the van Allen belt. Also, the orbit eccentricity of  $e \simeq 0.41$  is high enough to attain sufficient velocity differences for the KT experiment. Although the relatively high orbit reduces the in-orbit velocity of the satellite by a factor of 2.8 compared with a low-Earth circular orbit, it is still 20 times higher than for an Earth-based experiment.

### 5.2. Satellite bus structure and subsystems

The satellite has cylindrical shape, with a height and a diameter of about 1.5 m. It spins around its cylindrical axis which is always directed towards the Sun. The front facing the Sun is covered by solar panels. Behind the front plate serving as a thermal shield a cylindrical box for on-board electronics and thruster control is located. The experimental box whose temperature is actively controlled is placed below the electronics. A stringer structure below the experimental box carries the kick motor and the fuel tank. Four

clusters of ion thrusters for fine (drag-free) attitude control as well as three clusters of cold gas thrusters for coarse attitude control and first acquisition operation are mounted circumferentially. The structure elements of the entire bus have to satisfy the extreme requirement for passive thermal control. Their thermal expansion coefficient has to be less than  $10^{-6} \text{ K}^{-1}$ .

The total satellite mass is about 250 kg, including 90 kg of experimental payload. The total power budget is estimated to be less than 250 W.

*5.2.1. Attitude and orbit control.* During experimental and safe-mode coarse attitude and orbit control are based on a Sun sensor (1 arcsec resolution) and a star sensor (10 arcsec resolution). Fibre gyros are used for spin and de-spin manoeuvres and serve to control the cold gas thrusters. The fine attitude control, also called the drag-free control, must be carried out with an accuracy of  $10^{-10} \text{ m s}^{-2}$  within the signal bandwidth of  $10^{-2}$ – $10^{-3} \text{ Hz}$ , depending on the satellite's spin rate. The general principle of drag-free control is to make the satellite's trajectory as close as possible to a geodesic. Therefore, a capacitive reference sensor [21] is used. The sensor unit consists of a test mass whose movements are measured capacitively with respect to all six degrees of freedom. Apart from the sensing electrodes, electrodes for servo-control surround the test mass and compensate its movement relative to the satellite structure. The signal is also used to control the satellite's movement via the ion thrusters. Thus, the test mass falls quasi-freely and is shielded against all disturbances by the satellite, in particular against solar pressure and drag. Because the servo-control is influenced by back-action effects, the test mass and the servo-control form a spring–mass system whose spring constant and eigenfrequency must be adapted to the signal bandwidth. Therefore, electrode surfaces, charging by external sources as well as the precision of the test mass and the electrode alignments influence the measurement of the position directly and make necessary repeated in-orbit calibration manoeuvres [21]. The chosen orbit avoids charging effects as much as possible.

FEEP ion thrusters (field-emission electric propulsion) must be used to overcome (a) solar radiation pressure acting on the satellite and disturbing its free-fall behaviour and (b) to control the residual acceleration down to  $10^{-10} \text{ m s}^{-2}$  in the signal bandwidth. The first requirement sets an upper limit for the thrust: linear forces acting on the satellite are less than  $50 \mu\text{N}$  in all three axes and maximum torques are about  $10 \mu\text{Nm}$ . The second condition determines the resolution of thrust control which has to be done with an accuracy of about  $0.1 \mu\text{N}$ . A FEEP able to satisfy these requirements is the indium liquid metal ion source (LMIS) of the Austrian Research Centers Seibersdorf (ARCS) [22]. Thrust is produced by accelerating indium ions in a strong electrical field. A sharpened tungsten needle is mounted in the centre of a cylindrical indium reservoir bonded to a ceramic tube which houses a heater element for melting the indium. Ion emission is started by applying a high positive potential between the tip covered with a thin indium film and an accelerator electrode. To avoid charging a neutralizer emitting electrons is installed. The FEEPs have a length of 2 cm, a diameter of 4 mm, and weigh only several grams sufficient for the entire mission. A continuous thrust of  $1.5 \mu\text{N}$  per thruster is available. For a satellite diameter of about 1.5 m (the maximum ASAP 5 size), the solar radiation pressure of  $\sim 4.4 \mu\text{N m}^{-2}$  and the radiation pressure of the Earth albedo of  $1.2 \mu\text{N m}^{-2}$  sum up to a total drag of about  $10 \mu\text{N}$ . Considering thruster noise, misalignments and other disturbing effects, a continuous thrust of  $12 \mu\text{N}$  would be sufficient. To control all six degrees of freedom a minimum of three clusters of four thrusters is necessary. To guarantee a continuous thrust with some redundancy four clusters are desirable. The power consumption is less than 3 W on average with peaks up to 25 W.

## 6. Conclusion

The proposed OPTIS mission is capable to make considerable improvements, up to three orders of magnitude, in the tests of SR and GR. It is designed to be a low-cost mission. It is based on using: (a) recent laboratory developments in optical technology and (b) the advantages of space conditions: a quiet environment, long integration time, large velocities and large potential differences.

The optical technology includes an optical comb generator, stabilized lasers and highly stable cavities. We note that an alternative optical cavity system consisting of a monolithic silicon block operated at  $\sim 140$  K, the temperature where the thermal expansion coefficient vanishes, should be studied [23]. The advantage of this approach could be a significantly reduced level of creep and therefore a corresponding improvement of the KT test.

## References

- [1] Brillat A and Hall J L 1979 *Phys. Rev. Lett.* **42** 549
- [2] Hils D and Hall J L 1990 *Phys. Rev. Lett.* **64** 1697
- [3] Turneaure J P *et al* 1983 *Phys. Rev.* **27** 1705
- [4] Buchman S *et al* 1998 *Proc. IEEE Int. Frequency Symp.* (Piscataway, NJ: IEEE) p 534
- [5] Gambini R and Pullin J 1999 *Phys. Rev. D* **59** 124021
- [6] Ellis J, Mavromatos N E and Nanopoulos D V 1999 Probing models of quantum space–time foam *Preprint gr-qc/9909085*
- [7] Damour T and Polyakov A M 1994 *Nucl. Phys. B* **423** 532  
Damour T and Polyakov A M 1996 *Gen. Rel. Grav.* **12** 1171
- [8] Damour T 1997 Gravity, equivalence principle and clocks *Preprint gr-qc/9711060*
- [9] Damour T 2000 *Gravitational Waves and Experimental Gravity* ed J Trần Thanh Vân *et al* (Hanoi: World Publishers) p 357
- [10] Godone A, Novero C and Tavella P 1995 *Phys. Rev. D* **51** 319
- [11] Robertson H P 1949 *Rev. Mod. Phys.* **21** 378
- [12] Mansouri R and Sexl R U 1977 *Gen. Rel. Grav.* **8** 497  
Mansouri R and Sexl R U 1977 *Gen. Rel. Grav.* **8** 515  
Mansouri R and Sexl R U 1977 *Gen. Rel. Grav.* **8** 809
- [13] Lämmerzahl C and Haugan M P 2001 *Phys. Lett. A* **282** 223
- [14] Vessot R F C *et al* 1980 *Phys. Rev. Lett.* **45** 2081
- [15] Young B C, Cruz F C and Bergquist J C 1999 *Phys. Rev. Lett.* **82** 3799
- [16] Seel S *et al* 1997 *Phys. Rev. Lett.* **78** 4741
- [17] Storz R *et al* 1998 *Opt. Lett.* **23** 1031
- [18] Diddams S A *et al* 2000 *Phys. Rev. Lett.* **84** 5102
- [19] Reichert J *et al* 1999 *Opt. Commun.* **172** 59
- [20] 1998 LISA Pre-Phase A Report 2nd edn July pp 126–9
- [21] Touboul P 2001 *Gyroscopes, Clock, Interferometers, . . . : Testing Relativistic Gravity in Space* ed C Lämmerzahl, C W F Everitt and F W Hehl (Berlin: Springer) p 274
- [22] 2000 Austrian Research Centers, Seibersdorf ARCS Indium Liquid Metal Ion Source
- [23] Richard J P and Hamilton J J 1991 *Rev. Sci. Instrum.* **62** 2375